Simultaneous effects of magnetic field and space porosity on compressible Maxwell fluid transport induced by a surface acoustic wave in a microchannel

Khaled S. Mekheimer[a)b)], Soliman R. Komy[c)], and Sara I. Abdelsalam[d)†]

[a)] *Mathematics & Statistics Department, Faculty of Science, Taif University, Hawia* (888) *Taif, Saudi Arabia*
[b)] *Department of Mathematics, Faculty of Science (Men), Al-Azhar University, Nasr City, Cairo, Egypt*
[c)] *Department of Mathematics, Faculty of Science, Helwan University, Cairo, Egypt*
[d)] *Basic Science Department, Faculty of Engineering, The British University in Egypt, Al-Shorouk City, Misr-Suez Desert Road, P. O. Box* 43, *Cairo* 11837, *Egypt*

(Received 6 February 2013; revised manuscript received 5 May 2013)

Peristaltic motion induced by a surface acoustic wave of a viscous, compressible and electrically conducting Maxwell fluid in a confined parallel-plane microchannel through a porous medium is investigated in the presence of a constant magnetic field. The slip velocity is considered and the problem is discussed only for the free pumping case. A perturbation technique is employed to analyze the problem in terms of a small amplitude ratio. The phenomenon of a "backward flow" is found to exist in the center and at the boundaries of the channel. In the second order approximation, the net axial velocity is calculated for various values of the fluid parameters. Finally, the effects of the parameters of interest on the mean axial velocity, the reversal flow, and the perturbation function are discussed and shown graphically. We find that in the non-Newtonian regime, there is a possibility of a fluid flow in the direction opposite to the propagation of the traveling wave. This work is the most general model of peristalsis created to date with wide-ranging applications in biological, geophysical and industrial fluid dynamics.

Keywords: peristaltic flow, Maxwell fluid, porous medium, slip flow, microchannel

PACS: 47.40.−x, 47.45.Gx, 47.56.+r, 52.30.Cv **DOI:** 10.1088/1674-1056/22/12/124702

1. Introduction

Microchannels built in microelectro–mechanical systems (MEMS) are easily subjected to environmental noises, such as oscillations, vibrations or externally excited traveling waves (surface acoustic waves (SAW)).[1–5] Mekheimer and Abdel–Wahab[4] studied the effects of compressibility induced by a surface acoustic wave and wall compliance in a microchannel. They concluded that the mean flow increases with the compressibility parameter increasing. The latter one is related to the peristaltic motion since the walls are flexible. Recent progress in MEMS technology providesmicro-fluid system manufacture and application pluralism. Because the micro-fluid systems have the advantages of tiny size and are easy-to-carry, they also have high accuracy and a short response time. Experimental and theoretical results[6,7] show that the flow velocity of the gas is proportional to the second power of the SAW displacement velocity in these microchannels.

Molecular gases flowing in rigid channels with the dominant parameter being the Knudsen number ($K_n = A/l$, where A is the coefficient close to the mean free path of the gas and l is the width of the channel) have been considered by many researchers;[4,6,7] some of these researchers have started to investigate the slip flow ($0.001 \leq K_n < 0.15$) within a rigid corrugated-wall plane channel, which are common in the microdomains of MEMS applications.[8,9] Mekheimer and Abdel–Wahab[4] concluded that the slip parameter has a decreasing effect on the mean flow until the reversal flow occurs.

To extend our interest in the study of the flow of molecular gases in microdomains, we investigate what happens when a small-amplitude sinusoidal wave is assumed to travel down the wall of a two-dimensional (2D) microchannel of constant width but rather-long length where the velocity-slip effect is present. Other studies related to peristaltic pumping using perturbation techniques have been conducted on the assumption that the mean free path (l) of the molecular gases is much larger than the wave amplitude (a) along the flexible wall[6,7] together with the no-slip boundary condition.

Peristaltic transport is a form of fluid transport that occurs when a progressive wave of area contraction or expansion propagates along the length of an extensible tube containing a liquid. It appears to be a major mechanism for urine transport in ureter, food mixing and chyme movement in intestinal transport, the transport of spermatozoa in the cervical canal, the transport of bile in bile ducts, etc.[10–13] Technical roller and finger pumps also operate according to this rule.

It is known that non-Newtonian effects produce unexpected changes in fluid behavior through viscoelastic regimes. Here, we present a general description of peristaltic wave propagation that introduces a wide diversity of physical effects. It thus provides an ideal analytical platform for investigating phenomena such as back flow, which has been sug-

†Corresponding author. E-mail: sara.abdelsalam@bue.edu.eg, siabdelsalam@yahoo.com

© 2013 Chinese Physical Society and IOP Publishing Ltd

gested as a likely cause of vesicoureteral reflux in urology. Ali *et al.*[14] have studied the peristaltic flow of a Maxwell fluid in a channel with compliant walls; they found that the relaxation time has an increasing effect on the reversal flow. Elkoumy *et al.*[15] have studied peristaltic transport through a porous medium of a Maxwell model in the presence of a magnetic field and the Hall effect. They concluded that the relaxation time has a decreasing effect on the mean velocity distribution. Hayat *et al.*[16] studied the peristaltic flow of a Maxwell fluid in a porous medium in the presence of Hall effects.

Flow through a porous medium has been of considerable interest in recent years, particularly among geophysical fluid dynamicists. Some progress has been made in the presence of porous media. For recent contributions, we refer to some interesting studies in Refs. [17]–[21]. The most general study of the stimulation of a compressible fluid flow in porous medium via the peristaltic mechanism is presented in Ref. [22], which has been used as a starting point in order to include non-Newtonian effects into the peristaltic model.

The magnetohydrodynamic (MHD) flow of a fluid in a channel with elastic, rhythmically contracting walls (peristaltic flow) is of interest in connection with certain problems of the movement of conductive physiological fluids, e.g., blood, with the need for theoretical research on the operation of a peristaltic MHD compressor. Peristaltic motion of a third-order fluid under the effect of an induced magnetic field was studied by Hayat *et al.*[23] Also, Mekheimer[24,25] studied both the peristaltic flow of blood in the presence of a magnetic field and the magnetohydrodynamic peristaltic transport in an inclined channel. Mekheimer[24] concluded that the Hartmann number has an increasing effect on the flow rate.

Many studies have investigated the effects of different parameters on incompressible fluids through peristalsis, only a few articles have considered compressible fluids.[4,22,26] The latter one concluded that the compressibility of the liquid has a strong influence on the net flow induced. The aim of this article is to study the slip flow field generated by the wavy motion of a compressible Maxwell fluid in a microchannel in the presence of a constant magnetic field through a porous medium. We suppose that the compressible fluid inside the microchannel is originally stationary, i.e., the zeroth-order pressure gradient is neglected at the beginning. Our study here might be directly applied to the gas flowing in bronchiole or microbronchia.

We formulate the problem in Section 2. In Section 3, we solve the problem. The results and discussion as well as the conclusions are presented in Sections 4 and 5, respectively. We find that in the non-Newtonian regime, there is a possibility of a fluid flow in the direction opposite to the propagation of the traveling wave.

2. Formulation of the problem

We consider a viscous, compressible, and electrically conducting Maxwell fluid in a 2D symmetric channel of uniform width $2d$. The flow in the porous space is due to sinusoidal small-amplitude traveling waves on the flexible walls of the channel. A uniform magnetic field B_0 is acting along the y axis and the induced magnetic field is assumed to be negligible. We introduce the Cartesian coordinate system with the x axis along the centerline of the channel and the y axis normal to it. Let u and v denote the velocity components along the x and y directions, respectively.

The flow is governed by the continuity equation

$$\frac{\partial \rho}{\partial t} + (\boldsymbol{V}\cdot\boldsymbol{\nabla}\rho) + \rho(\boldsymbol{\nabla}\cdot\boldsymbol{V}) = 0, \tag{1}$$

and the equations of motion

$$\rho\frac{\partial \boldsymbol{V}}{\partial t} + \rho(\boldsymbol{V}\cdot\boldsymbol{\nabla})\boldsymbol{V} = -\boldsymbol{\nabla}p + \boldsymbol{\nabla}\cdot\boldsymbol{S} + \boldsymbol{R} + \boldsymbol{J}\times\boldsymbol{B} + \frac{\mu}{3}\boldsymbol{\nabla}(\boldsymbol{\nabla}\cdot\boldsymbol{V}), \tag{2}$$

where ρ, t, p, and μ are the density of fluid, time, the interaction pressure due to the motion of fluid on the wall, and the dynamic viscosity, respectively; $\boldsymbol{V}$, $\boldsymbol{J}$, and $\boldsymbol{B}$ are the velocity vector, electric current density, and magnetic induction vector, respectively.

The extra stress tensor $\boldsymbol{S}$ for the linear Maxwell fluid is defined as[14]

$$\left(1+\tau\frac{\partial}{\partial t}\right)\boldsymbol{S} = \mu(\boldsymbol{\nabla}\boldsymbol{V} + \boldsymbol{\nabla}\boldsymbol{V}^{\mathrm{T}}), \tag{3}$$

where τ is the relaxation time and $\boldsymbol{R}$ is the Darcy resistance for a fluid in a porous medium. The Darcy resistance in a Maxwell fluid is defined by[16]

$$\left(1+\tau\frac{\partial}{\partial t}\right)\boldsymbol{R} = -\frac{\mu}{W}\boldsymbol{V}, \tag{4}$$

where W is the permeability parameter. The conducting fluid is permeated by an imposed uniform magnetic field B_0, which acts in the transverse direction. For a low magnetic Reynolds number, the induced magnetic field can be ignored, the magnetic body force $\boldsymbol{J}\times\boldsymbol{B}$ becomes $\sigma(\boldsymbol{V}\times\boldsymbol{B})\times\boldsymbol{B}$ when imposed, induced electric fields are negligible and only the magnetic field $\boldsymbol{B}$ contributes to the current $\boldsymbol{J} = \sigma(\boldsymbol{V}\times\boldsymbol{B})$. Here, σ is the electrical conductivity of the fluid.

The characteristic response of the fluid to a compression is described by the constitutive equation

$$\frac{1}{\rho}\frac{\partial \rho}{\partial t} = k_{\mathrm{c}}, \tag{5}$$

where k_{c} is the compressibility of the liquid. The solution of Eq. (5) for the density as a function of pressure is given by

$$\rho = \rho_0 \exp(k_{\mathrm{c}}(p - p_{\mathrm{c}})), \tag{6}$$

where ρ_0 is the (constant) density at the reference pressure p_{c}.

The continuity equation will take the form

$$\frac{\partial \rho}{\partial t} + u\frac{\partial \rho}{\partial x} + v\frac{\partial \rho}{\partial y} + \rho\left(\frac{\partial u}{\partial x} + \frac{\partial v}{\partial y}\right) = 0, \tag{7}$$

and

$$\left(1+\tau\frac{\partial}{\partial t}\right)\rho\left(\frac{\partial u}{\partial t}+u\frac{\partial u}{\partial x}+v\frac{\partial u}{\partial y}\right)\frac{\partial}{\partial y}$$
$$=-\left(1+\tau\frac{\partial}{\partial t}\right)\frac{\partial p}{\partial x}+\mu\nabla^2 u-\frac{\mu}{W}u-\sigma B_0^2\left(1+\tau\frac{\partial}{\partial t}\right)u$$
$$+\frac{\mu}{3}\left(1+\tau\frac{\partial}{\partial t}\right)\left(\frac{\partial u}{\partial x}+\frac{\partial v}{\partial y}\right), \tag{8}$$
$$\left(1+\tau\frac{\partial}{\partial t}\right)\rho\left(\frac{\partial v}{\partial t}+u\frac{\partial v}{\partial x}+v\frac{\partial v}{\partial y}\right)$$
$$=-\left(1+\tau\frac{\partial}{\partial t}\right)\frac{\partial p}{\partial y}+\mu\nabla^2 v-\frac{\mu}{W}v$$
$$+\frac{\mu}{3}\left(1+\tau\frac{\partial}{\partial t}\right)\left(\frac{\partial u}{\partial x}+\frac{\partial v}{\partial y}\right), \tag{9}$$

where x and y are the Cartesian coordinates with x measured in the direction of wave propagation and y measured in the direction normal to the mean position of the walls.

Let the vertical displacements of the upper and lower walls be η and $-\eta$, respectively, such that

$$\eta(x,t)=a\cos\left(\frac{2\pi}{\lambda}(x-ct)\right), \tag{10}$$

where a is the amplitude, λ is the wave length, and c is the wave speed. The horizontal displacement will be assumed to be zero. Together with the slip boundary condition at the wall, the boundary conditions can be written as

$$u(x,\pm d\pm\eta,t)=\mp A\frac{\partial u}{\partial y}, \tag{11}$$

for the slip boundary condition and

$$v(x,\pm d\pm\eta,t)=\pm\frac{\partial\eta(x,t)}{\partial t}, \tag{12}$$

for the no permeability condition.

By using the following nondimensional variables and parameters where c and d are the characteristics velocity and length:

$$x^*=\frac{x}{d},\ y^*=\frac{y}{d},\ \eta^*=\frac{\eta}{d},\ u^*=\frac{u}{c},\ v^*=\frac{v}{c},\ \rho^*=\frac{\rho}{\rho_0},$$
$$t^*=\frac{ct}{d},\ W^*=\frac{W}{d^2},\ p^*=\frac{p}{\rho_0 c^2},\ p_c^*=\frac{p_c}{\rho_0 c^2},\ \tau^*=\frac{\tau c}{d}, \tag{13}$$

the dimensionless parameters are obtained as

$$\varepsilon=\frac{a}{d},\ \alpha=\frac{2\pi d}{\lambda},\ R=\frac{\rho_0 cd}{\mu},\ \chi=k_c\rho_0 c^2,\ \text{and}\ M=\frac{d\sigma}{\rho_0 c}B_0^2,$$

which represent the amplitude ratio, the wave number, Reynolds number, the compressibility parameter, and the magnetic parameter, respectively.

In terms of these variables, Eqs. (6)–(12) reduce to

$$\rho=\exp(\chi(p-p_c)), \tag{14}$$
$$\frac{\partial\rho}{\partial t}+u\frac{\partial\rho}{\partial x}+v\frac{\partial\rho}{\partial y}+\rho\left(\frac{\partial u}{\partial x}+\frac{\partial v}{\partial y}\right)=0, \tag{15}$$
$$\left(1+\tau\frac{\partial}{\partial t}\right)\rho\left(\frac{\partial u}{\partial t}+u\frac{\partial u}{\partial x}+v\frac{\partial u}{\partial y}\right)$$
$$=-\left(1+\tau\frac{\partial}{\partial t}\right)\frac{\partial p}{\partial x}+\frac{1}{R}\nabla^2 u-\frac{1}{RW}u$$
$$-M\left(1+\tau\frac{\partial}{\partial t}\right)u+\frac{1}{3R}\left(1+\tau\frac{\partial}{\partial t}\right)\frac{\partial}{\partial x}\left(\frac{\partial u}{\partial x}+\frac{\partial v}{\partial y}\right), \tag{16}$$
$$\left(1+\tau\frac{\partial}{\partial t}\right)\rho\left(\frac{\partial v}{\partial t}+u\frac{\partial v}{\partial x}+v\frac{\partial v}{\partial y}\right)$$
$$=-\left(1+\tau\frac{\partial}{\partial t}\right)\frac{\partial p}{\partial y}+\frac{1}{R}\nabla^2 v-\frac{1}{RW}v$$
$$+\frac{1}{3R}\left(1+\tau\frac{\partial}{\partial t}\right)\frac{\partial}{\partial y}\left(\frac{\partial u}{\partial x}+\frac{\partial v}{\partial y}\right), \tag{17}$$
$$\eta=\varepsilon\cos\alpha(x-t), \tag{18}$$
$$u(x,\pm1\pm\eta,t)=\mp K_n\frac{\partial u}{\partial y}, \tag{19}$$
$$v(x,\pm1\pm\eta,t)=\pm\frac{\partial\eta}{\partial t}, \tag{20}$$

in which the asterisks have been suppressed for simplicity.

3. Method of solution

To solve the system of Eqs. (12)–(15), we first take the steady parallel flow case in which $u=u_0(y)$ and $v=0$. So, under the effect of a constant pressure gradient $\partial p/\partial x=\partial p_0/\partial x=$ constant, the solution of the system will be

$$u_0(y)=\frac{R}{\lambda_1^2}\frac{\mathrm{d}p_0}{\mathrm{d}x}\frac{(\cosh\lambda_1 y-\cosh\lambda_1-K_n\lambda_1\sinh\lambda_1)}{(\cosh\lambda_1+K_n\lambda_1\sinh\lambda_1)}, \tag{21}$$

with $\lambda_1=\sqrt{MR+1/W}$.

For the no-slip condition, we have $K_n\to 0$ and so

$$u_0(y)=\frac{R}{\lambda_1^2}\frac{\mathrm{d}p_0}{\mathrm{d}x}\frac{(\cosh\lambda_1 y-\cosh\lambda_1)}{\cosh\lambda_1}. \tag{22}$$

In the steady state situation, the traveling wave motion in the wall will create a peristaltic mean flow. This mean flow depends on the physical quantities relevant to the motion of the system. The case of pure peristalsis, $\partial p_0/\partial x=0$ has been termed "free pumping" by Fung and Yih.[27] Although the mean peristaltic motion is caused by a single harmonic wave number α, the details of the flow are quite complicated because of the nonlinearity in the governing equations. We assume the pressure, the velocity components and the density in the following forms:

$$p=\varepsilon p_1(x,y,t)+\varepsilon^2 p_2(x,y,t)+\cdots,$$
$$u=\varepsilon u_1(x,y,t)+\varepsilon^2 u_2(x,y,t)+\cdots,$$
$$v=\varepsilon v_1(x,y,t)+\varepsilon^2 v_2(x,y,t)+\cdots,$$
$$\rho=1+\varepsilon\rho_1(x,y,t)+\varepsilon^2\rho_2(x,y,t)+\cdots. \tag{23}$$

Substituting expansions (23) into Eqs. (14)–(17) and equating the coefficients of equal powers of ε on both sides of the equations, we obtain for ε

$$\rho_1=\chi p_1,\quad \frac{\partial\rho_1}{\partial t}+\frac{\partial u_1}{\partial x}+\frac{\partial v_1}{\partial y}=0,$$
$$\left(1+\tau\frac{\partial}{\partial t}\right)\frac{\partial u_1}{\partial t}=-\left(1+\tau\frac{\partial}{\partial t}\right)\frac{\partial p_1}{\partial x}+\frac{1}{R}\left(\frac{\partial^2 u_1}{\partial x^2}+\frac{\partial^2 u_1}{\partial y^2}\right)$$
$$-\frac{1}{RW}u_1-M\left(1+\tau\frac{\partial}{\partial t}\right)u_1$$
$$+\frac{1}{3R}\left(1+\tau\frac{\partial}{\partial t}\right)\frac{\partial}{\partial x}\left(\frac{\partial u_1}{\partial x}+\frac{\partial v_1}{\partial y}\right),$$
$$\left(1+\tau\frac{\partial}{\partial t}\right)\frac{\partial v_1}{\partial t}=-\left(1+\tau\frac{\partial}{\partial t}\right)\frac{\partial p_1}{\partial y}+\frac{1}{R}\left(\frac{\partial^2 v_1}{\partial x^2}+\frac{\partial^2 v_1}{\partial y^2}\right)$$

$$-\frac{1}{RW}v_1+\frac{1}{3R}\Big(1+\tau\frac{\partial}{\partial t}\Big)\frac{\partial}{\partial y}\times\Big(\frac{\partial u_1}{\partial x}+\frac{\partial v_1}{\partial y}\Big); \tag{24}$$

for ε^2

$$\rho_2=\chi p_2+\frac{1}{2}\chi^2 p_1^2,$$

$$\frac{\partial\rho_2}{\partial t}+u_1\frac{\partial\rho_1}{\partial x}+v_1\frac{\partial\rho_1}{\partial y}+\frac{\partial u_2}{\partial x}+\frac{\partial v_2}{\partial y}+\rho_1\Big(\frac{\partial u_1}{\partial x}+\frac{\partial v_1}{\partial y}\Big)=0,$$

$$\Big(1+\tau\frac{\partial}{\partial t}\Big)\Big(\frac{\partial u_2}{\partial t}+u_1\frac{\partial u_1}{\partial x}+v_1\frac{\partial u_1}{\partial y}+\rho_1\frac{\partial u_1}{\partial t}\Big)$$
$$=-\Big(1+\tau\frac{\partial}{\partial t}\Big)\frac{\partial p_2}{\partial x}+\frac{1}{R}\Big(\frac{\partial^2 u_2}{\partial x^2}+\frac{\partial^2 u_2}{\partial y^2}\Big)-\frac{1}{RW}u_2$$
$$-M\Big(1+\tau\frac{\partial}{\partial t}\Big)u_2+\frac{1}{3R}\Big(1+\tau\frac{\partial}{\partial t}\Big)\frac{\partial}{\partial x}\Big(\frac{\partial u_2}{\partial x}+\frac{\partial v_2}{\partial y}\Big),$$

$$\Big(1+\tau\frac{\partial}{\partial t}\Big)\Big(\frac{\partial v_2}{\partial t}+u_1\frac{\partial v_1}{\partial x}+v_1\frac{\partial v_1}{\partial y}+\rho_1\frac{\partial v_1}{\partial t}\Big)$$
$$=-\Big(1+\tau\frac{\partial}{\partial t}\Big)\frac{\partial p_2}{\partial y}+\frac{1}{R}\Big(\frac{\partial^2 v_1}{\partial x^2}+\frac{\partial^2 v_1}{\partial y^2}\Big)-\frac{1}{RW}v_1$$
$$+\frac{1}{3R}\Big(1+\tau\frac{\partial}{\partial t}\Big)\frac{\partial}{\partial y}\Big(\frac{\partial u_2}{\partial x}+\frac{\partial v_2}{\partial y}\Big), \tag{25}$$

etc.

We represent the boundary conditions (19) and (20) by a Taylor expansion around $y=\pm1$, i.e.,

$$u(x,\pm1\pm\eta,t)=u(x,\pm1,t)\pm\eta(x,t)u_y(x,\pm1,t)+\frac{\eta^2}{2}u_{yy}(x,\pm1,t)+\cdots,$$
$$v(x,\pm1\pm\eta,t)=v(x,\pm1,t)\pm\eta(x,t)v_y(x,\pm1,t)+\frac{\eta^2}{2}v_{yy}(x,\pm1,t)+\cdots. \tag{26}$$

Substituting expansions (26) into Eqs. (19) and (20), then using expansion (23) and expressing cosines and sines in exponential powers, we obtain that for ε

$$u_1(x,\pm1,t)=\mp K_n u_{1y}(x,\pm1,t), \tag{27}$$
$$v_1(x,\pm1,t)=\mp\frac{\mathrm{i}\alpha}{2}(\mathrm{e}^{\mathrm{i}\alpha(x-t)}-\mathrm{e}^{-\mathrm{i}\alpha(x-t)}), \tag{28}$$

for ε^2

$$u_2(x,\pm1,t)\pm\frac{1}{2}(\mathrm{e}^{\mathrm{i}\alpha(x-t)}+\mathrm{e}^{-\mathrm{i}\alpha(x-t)})u_{1y}(x,\pm1,t)$$
$$=\mp K_n\Big[u_{2y}(x,\pm1,t)\pm\frac{1}{2}(\mathrm{e}^{\mathrm{i}\alpha(x-t)}+\mathrm{e}^{-\mathrm{i}\alpha(x-t)})\times u_{1yy}(x,\pm1,t)\Big], \tag{29}$$

$$v_2(x,\pm1,t)\pm\frac{1}{2}\big(\mathrm{e}^{\mathrm{i}\alpha(x-t)}+\mathrm{e}^{-\mathrm{i}\alpha(x-t)}\big)v_{1y}(x,\pm1,t)=0. \tag{30}$$

Note that we do not need the third boundary condition in this order.

Examination of Eqs. (24)–(26) shows that we can seek a solution in the following forms:

$$u_1(x,y,t)=U_1(y)\mathrm{e}^{\mathrm{i}\alpha(x-t)}+\overline{U}_1(y)\mathrm{e}^{-\mathrm{i}\alpha(x-t)},$$
$$v_1(x,y,t)=V_1(y)\mathrm{e}^{\mathrm{i}\alpha(x-t)}+\overline{V}_1(y)\mathrm{e}^{-\mathrm{i}\alpha(x-t)},$$
$$p_1(x,y,t)=P_1(y)\mathrm{e}^{\mathrm{i}\alpha(x-t)}+\overline{P}_1(y)\mathrm{e}^{-\mathrm{i}\alpha(x-t)},$$
$$\rho_1(x,y,t)=\chi P_1(y)\mathrm{e}^{\mathrm{i}\alpha(x-t)}+\chi\overline{P}_1(y)\mathrm{e}^{-\mathrm{i}\alpha(x-t)}, \tag{31}$$

and

$$u_2(x,y,t)=U_{20}(y)+U_2(y)\mathrm{e}^{2\mathrm{i}\alpha(x-t)}+\overline{U}_2(y)\mathrm{e}^{-2\mathrm{i}\alpha(x-t)},$$
$$v_2(x,y,t)=V_{20}(y)+V_2(y)\mathrm{e}^{2\mathrm{i}\alpha(x-t)}+\overline{V}_2(y)\mathrm{e}^{-2\mathrm{i}\alpha(x-t)},$$
$$p_2(x,y,t)=P_{20}(y)+P_2(y)\mathrm{e}^{2\mathrm{i}\alpha(x-t)}+\overline{P}_2(y)\mathrm{e}^{-2\mathrm{i}\alpha(x-t)},$$
$$\rho_2(x,y,t)=D_{20}(y)+D_2(y)\mathrm{e}^{2\mathrm{i}\alpha(x-t)}+\overline{D}_2(y)\mathrm{e}^{-2\mathrm{i}\alpha(x-t)}. \tag{32}$$

Here, the overline denotes the complex conjugate.

Substituting Eq. (31) into Eqs. (24), (27), and (28), we obtain the following set of equations:

$$V_1'+\mathrm{i}\alpha U_1=\mathrm{i}\alpha\chi P_1,$$
$$-\mathrm{i}\alpha\gamma_1U_1=-\mathrm{i}\alpha\gamma_1P_1+\frac{1}{R}\Big[U''_1-\Big(\alpha^2+\frac{1}{W}+MR\gamma_1\Big)U_1\Big]+\frac{\mathrm{i}\alpha\gamma_1}{3R}(V_1'+\mathrm{i}\alpha U_1),$$
$$-\mathrm{i}\alpha\gamma_1V_1=-\gamma_1P_1'+\frac{1}{R}\Big[V_1''-\Big(\alpha^2+\frac{1}{W}\Big)V_1\Big]+\frac{\gamma_1}{3R}\frac{\mathrm{d}}{\mathrm{d}y}(V_1'+\mathrm{i}\alpha U_1),$$
$$U_1(\pm1)=\mp K_nU_1'(\pm1),\quad V_1(\pm1)=\mp\frac{\mathrm{i}\alpha}{2}, \tag{33}$$

where $\gamma_1=1-\mathrm{i}\alpha\tau$.

The set of equations for $\overline{U_1}$, $\overline{V_1}$, and $\overline{P_1}$ is conjugate to their counterparts in Eq. (33) so that it need not be written out explicitly. First, the system of Eq. (33) is solved. Substitution of the first expression of Eq. (33) into the second and third expressions yields

$$-\gamma^*P_1-\frac{\mathrm{i}}{\alpha}(U_1''-\beta^2U_1)=0,\quad -\gamma^*P_1'+(V_1''-\beta_1^2V_1)=0, \tag{34}$$

where the complex parameters $\gamma*$, γ, β, and β_1 are given by

$$\gamma*=\gamma_1\gamma,\quad \gamma=R-\frac{\mathrm{i}\alpha\chi}{3},$$
$$\beta^2=\alpha^2-\mathrm{i}\alpha\gamma_1R+\frac{1}{W}+MR\gamma_1,$$
$$\beta_1^2=\alpha^2-\mathrm{i}\alpha\gamma_1R+\frac{1}{W}, \tag{35}$$

with U_1 eliminated by the first expression of Eq. (33), we rewrite Eq. (34) as

$$-\frac{\mathrm{i}\chi}{\alpha}\Big[P_1''-\Big(\beta^2+\frac{\mathrm{i}\alpha\gamma*}{\chi}\Big)P_1\Big]+\frac{1}{\alpha^2}\frac{\mathrm{d}}{\mathrm{d}y}(V_1''-\beta^2V_1)=0. \tag{36}$$

Differentiating Eq. (36) with respect to y and using the first expression of Eq. (34) to express the derivatives of P_1 in terms of V_1 and its derivatives, we have the following equation:

$$\Gamma V_1^{(4)}-\Gamma\Big(\beta^2+\upsilon^2\Big)V_1''+\Gamma\beta_1^2\upsilon_1^2V_1=0, \tag{37}$$

where the complex parameters Γ, υ, and υ_1 are given by

$$\Gamma=1-\frac{\mathrm{i}\alpha\chi}{\gamma*},\quad \upsilon^2=\beta_1^2-\frac{(\beta_1^2-\alpha^2)}{\Gamma},$$
$$\upsilon^2=\beta^2-\frac{(\beta^2-\alpha^2)}{\Gamma}. \tag{38}$$

By using Eq. (35), the expressions in Eq. (38) for υ and υ_1 can be written in terms of γ_1, R, τ, and χ as

$$\upsilon^2 = \frac{-\frac{\mathrm{i}}{3}\alpha^3\chi(4-\mathrm{i}\alpha\tau)+\alpha^2 R(1-\chi)(1-\mathrm{i}\alpha\tau)-\frac{\mathrm{i}\alpha\chi}{W}}{R(1-\mathrm{i}\alpha\tau)-\frac{\mathrm{i}\alpha\chi}{3}(4-\mathrm{i}\alpha\tau)},$$
$$\upsilon_1^2 = \frac{-\frac{\mathrm{i}}{3}\alpha^3\chi(4-\mathrm{i}\alpha\tau)+\alpha^2 R(1-\chi)(1-\mathrm{i}\alpha\tau)-\frac{\mathrm{i}\alpha\chi}{W}-\mathrm{i}\alpha\chi MR(1-\mathrm{i}\alpha\tau)}{R(1-\mathrm{i}\alpha\tau)-\frac{\mathrm{i}\alpha\chi}{3}(4-\mathrm{i}\alpha\tau)}. \quad (39)$$

Notice that if $M=0$, then $\upsilon^2=\upsilon_1^2$. In addition, if $\tau=0$ and $W\to\infty$, then υ^2 of Mekheimer and Abdel–Wahab[4] is recovered. Also notice that $\upsilon=\upsilon_1=\alpha$ for $\chi=0$, i.e., for incompressible liquids. Clearly, the boundary conditions, i.e., the fifth expression of Eq. (33), demand that $V_1(y)$ be odd in y, hence the solution for V_1 is given by

$$V_1(y) = C_1\sinh a_1 y + C_2\sinh a_2 y, \quad (40)$$

where C_1 and C_2 are complex constants; a_1 and a_2 are given by

$$a_1^2 = \frac{(\beta^2+\upsilon^2)+\sqrt{(\beta^2+\upsilon^2)^2-4\beta_1^2\upsilon_1^2}}{2},$$
$$a_2^2 = \frac{(\beta^2+\upsilon^2)-\sqrt{(\beta^2+\upsilon^2)^2-4\beta_1^2\upsilon_1^2}}{2}. \quad (41)$$

Substitution of expression (40) into the second expression of Eq. (34) yields

$$\gamma^* P_1' = C_1(a_1^2-\beta_1^2)\sinh a_1 y + C_2(a_2^2-\beta_1^2)\sinh a_2 y. \quad (42)$$

It is easily seen that

$$P_1(y) = C_1\frac{(a_1^2-\beta_1^2)}{\gamma^* a_1}\cosh a_1 y + C_2\frac{(a_2^2-\beta_1^2)}{\gamma^* a_2}\cosh a_2 y + C_3, \quad (43)$$

where C_3 is a complex constant. Substitution of Eqs. (40) and (43) into the first expression of Eq. (33) yields

$$U_1(y) = b_1 C_1\cosh a_1 y + b_2 C_2\cosh a_2 y + C_3\chi, \quad (44)$$

where the complex constants b_1 and b_2 are given by

$$b_1 = \chi\frac{(a_1^2-\beta_1^2)}{\gamma^* a_1}+\frac{\mathrm{i}a_1}{\alpha}, \quad b_2 = \chi\frac{(a_2^2-\beta_1^2)}{\gamma^* a_2}+\frac{\mathrm{i}a_2}{\alpha}. \quad (45)$$

Finally, from the first expression of Eq. (34), we deduce that

$$C_3 = 0. \quad (46)$$

The boundary conditions, i.e., the fourth and fifth expressions of Eq. (33) then require

$$C_1 = \frac{\mathrm{i}\alpha}{2}\frac{b_2 g_2}{G}, \quad C_2 = -\frac{\mathrm{i}\alpha}{2}\frac{1}{\sinh a_2}\left(1+\frac{\sinh a_1}{G}b_2 g_2\right), \quad (47)$$

where

$$g_1 = \cosh a_1 + K_n a_1\sinh a_1, \quad g_2 = \cosh a_2 + K_n a_2\sinh a_2,$$

and

$$G = b_1 g_1\sinh a_2 - b_2 g_2\sinh a_1.$$

Thus, the first-order approximations of the velocity and pressure are described by Eqs. (40) and (43)–(47).

By substituting Eq. (32) into the first–fourth expressions of Eq. (25) with the aid of Eqs. (29) and (30), we obtain the following second-order set of equations:

$$D_{20} = \chi P_{20} + \chi^2\overline{P_1}P_1,$$
$$-P_{20}' + \frac{4}{3\mathrm{R}}V''_{20} - \frac{1}{RW}V_{20} = \mathrm{i}\alpha\chi P_1\overline{V_1} - \mathrm{i}\alpha\overline{P_1}V_1 + V_1\overline{V_1'} + V_1'\overline{V_1} - \mathrm{i}\alpha U_1\overline{V_1} + \mathrm{i}\alpha\overline{U}_1 V_1,$$
$$\frac{1}{R}U''_{20} - \left(\frac{1}{RW}+M\right)U_{20} = \mathrm{i}\alpha\chi\overline{U_1}P_1 - \mathrm{i}\alpha\chi\overline{P}_1 U_1 + V_1\overline{U_1'} + \overline{V_1}U_1',$$
$$V_{20}' = -\chi\left(P_1\overline{V_1'} + \overline{P}_1 V_1' + V_1\overline{P_1'} + \overline{V_1}P_1'\right),$$
$$U_{20}(\pm1) \pm \frac{1}{2}\left(\overline{U_1'}(\pm1) + U_1'(\pm1)\right) = \mp K_n\left[U_{20}'(\pm1) \pm \frac{1}{2}\left(\overline{U_1''}(\pm1) + U_1''(\pm1)\right)\right],$$
$$V_{20}(\pm1) \pm \frac{1}{2}\left(\overline{V_1'}(\pm1) + V_1'(\pm1)\right) = 0. \quad (48)$$

It will be seen that, as far as the net flow is concerned, only the functions U_{20}, V_{20}, P_{20}, and D_{20} participate in the solution, as long as terms up to $O(\varepsilon^2)$ are retained. Thus, the functions U_2, V_2, P_2, and D_2 do not contribute to the net flow and therefore, we shall not write down the equations that these functions satisfy, nor solve them. We continue with the solutions for P_{20},V_{20}, and U_{20}.

We rewrite the second–fourth expressions of Eq. (48), respectively, as

$$-P_{20}' + \frac{4}{3\mathrm{R}}V''_{20} - \frac{1}{RW}V_{20} = F,$$
$$U''_{20} - \left(\frac{1}{W}+MR\right)U_{20} = RL, \quad V_{20}' = -\chi H, \quad (49)$$

where the functions F, L, and H, corresponding to the right-hand sides of the second–fourth expressions of Eq. (49), are given by

$$F = \mathrm{i}\alpha\chi P_1\overline{V_1} - \mathrm{i}\alpha\overline{P_1}V_1 + V_1\overline{V_1'} + V_1'\overline{V_1} - \mathrm{i}\alpha U_1\overline{V_1} + \mathrm{i}\alpha\overline{U}_1 V_1,$$
$$L = \frac{\mathrm{d}}{\mathrm{d}y}\left(V_1\overline{U_1} + \overline{V_1}U_1\right), \quad H = \frac{\mathrm{d}}{\mathrm{d}y}\left(P_1\overline{V_1} + \overline{P}_1 V_1\right). \quad (50)$$

Here, the first expression of Eq. (33) is used to eliminate P_1 in function L. With H given by the third expression of Eq. (50), it is easily seen that the solution for V_{20} is given by

$$V_{20} = -\chi\left(P_1\overline{V_1} + \overline{P}_1 V_1\right) + D_1, \quad (51)$$

where the complex constant D_1 follows from the boundary condition, i.e., the sixth expression of Eq. (48).

Eliminating V_1' by the first expression of Eq. (33) and us-

ing the fourth and fifth expressions of Eq. (33) lead to

$$D_1 = \frac{\mathrm{i}\alpha}{2} K_n \left(\overline{U_1'}(1) - U_1'(1)\right). \tag{52}$$

Notice that $D_1 = 0$ at $K_n = 0$ (as indicated by Aarts and Ooms[22]) and hence $V_{20} = 0$ for $\chi = 0$, i.e., for incompressible liquids. With L given by the second expression of Eq. (50), it is easily seen that the solution for U_{20} is given by

$$U_{20}(y) = D_2 \cosh\lambda_1 y + D_3 \sinh\lambda_1 y + E(y), \tag{53}$$

where

$$\begin{aligned} E(y) = R\Big\{ & \frac{j_1}{(a_1+\overline{a_1})^2 - \lambda_1^2} \cosh(a_1+\overline{a_1})y \\ & + \frac{j_{11}}{(a_1-\overline{a_1})^2 - \lambda_1^2} \cosh(a_1-\overline{a_1})y \\ & + \frac{j_2}{(a_1+\overline{a_2})^2 - \lambda_1^2} \cosh(a_1+\overline{a_2})y \\ & + \frac{j_{22}}{(a_1-\overline{a_2})^2 - \lambda_1^2} \cosh(a_1-\overline{a_2})y \\ & + \frac{j_3}{(a_2+\overline{a_1})^2 - \lambda_1^2} \cosh(a_2+\overline{a_1})y \\ & + \frac{j_{33}}{(a_2-\overline{a_1})^2 - \lambda_1^2} \cosh(a_2-\overline{a_1})y \\ & + \frac{j_4}{(a_2+\overline{a_2})^2 - \lambda_1^2} \cosh(a_2+\overline{a_2})y \\ & + \frac{j_{44}}{(a_2-\overline{a_2})^2 - \lambda_1^2} \cosh(a_2-\overline{a_2})y \Big\}. \end{aligned} \tag{54}$$

The constants D_2 and D_3 are given by the fifth expression in Eq. (48) as

$$\begin{aligned} D_2 = {} & \frac{-1}{2(\cosh\lambda_1 + K_n\lambda_1\sinh\lambda_1)} \big[K_n\big(E'(1) - E'(-1)\big) \\ & + K_n(\beta_4 - \beta_5) + \beta_2 + \beta_3 + E(1) + E(-1)\big], \\ D_3 = {} & \frac{-1}{2(\sinh\lambda_1 + K_n\lambda_1\cosh\lambda_1)} \big[K_n\big(E'(1) + E'(-1)\big) \\ & + K_n\Big(\beta_4 + \beta_5\Big) + \beta_2 - \beta_3 + E(1) - E(-1)\big], \end{aligned} \tag{55}$$

where

$$\beta_2 = \frac{1}{2}\big(U_1'(1) + \overline{U_1'}(1)\big), \quad \beta_3 = -\frac{1}{2}\big(U_1'(-1) + \overline{U_1'}(-1)\big),$$

$$\beta_4 = \frac{1}{2}\big(U''_1(1) + \overline{U_1''}(1)\big), \quad \beta_5 = -\frac{1}{2}\big(U''_1(-1) + \overline{U_1''}(-1)\big),$$

and

$$j_1 = \frac{1}{2}(a_1C_1\overline{b_1C_1} + \overline{a_1}\,\overline{C_1}b_1C_1 + \overline{a_1}\,\overline{b_1C_1}C_1 + a_1b_1C_1\overline{C_1}),$$

$$j_2 = \frac{1}{2}(a_1C_1\overline{b_2C_2} + \overline{a_2}\,\overline{C_2}b_1C_1 + \overline{a_2}\,\overline{b_2C_2}C_1 + a_1b_1C_1\overline{C_2}),$$

$$j_3 = \frac{1}{2}(a_2C_2\overline{b_1C_1} + \overline{a_1}\,\overline{C_1}b_2C_2 + \overline{a_1}\,\overline{b_1C_1}C_2 + a_2b_2C_2\overline{C_1}),$$

$$j_4 = \frac{1}{2}(a_2C_2\overline{b_2C_2} + \overline{a_2}\,\overline{C_2}b_2C_2 + \overline{a_2}\,\overline{b_2C_2}C_2 + a_2b_2C_2\overline{C_2}),$$

$$j_{11} = \frac{1}{2}(a_1C_1\overline{b_1C_1} + \overline{a_1}\,\overline{C_1}b_1C_1 - \overline{a_1}\,\overline{b_1C_1}C_1 - a_1b_1C_1\overline{C_1}),$$

$$j_{22} = \frac{1}{2}(a_1C_1\overline{b_2C_2} + \overline{a_2}\,\overline{C_2}b_1C_1 - \overline{a_2}\,\overline{b_2C_2}C_1 - a_1b_1C_1\overline{C_2}),$$

$$j_{33} = \frac{1}{2}(a_2C_2\overline{b_1C_1} + \overline{a_1}\,\overline{C_1}b_2C_2 - \overline{a_1}\,\overline{b_1C_1}C_2 - a_2b_2C_2\overline{C_1}),$$

$$j_{44} = \frac{1}{2}(a_2C_2\overline{b_2C_2} + \overline{a_2}\,\overline{C_2}b_2C_2 - \overline{a_2}\,\overline{b_2C_2}C_2 - a_2b_2C_2\overline{C_2}).$$

Finally, it is easily seen that the solution for P_{20} is given by

$$P_{20}(y) = D_4 - \frac{4\chi}{3R}H(y) - \frac{1}{RW}\int_{-1}^{y} V_{20}(r)\,\mathrm{d}r - \int_{-1}^{y} F(r)\,\mathrm{d}r, \tag{56}$$

where the complex constant $D_4 = P_{20}(-1) + 4\chi H(-1)/3R$ follows from a given pressure $P_{20}(-1)$ on the channel wall.

Next, the net axial velocity is considered over one period of time. The average of a variable g over one period T of time t is

$$\langle g\rangle = \frac{1}{T}\int_0^T g(x,y,t)\,\mathrm{d}t, \tag{57}$$

where $T = 2\pi/\alpha$. Consequently, the mean net axial velocity $\langle u\rangle$ reads

$$\langle u\rangle = \varepsilon^2 U_{20}(y). \tag{58}$$

By neglecting the terms of $O(\varepsilon^3)$, the net flow rate $\langle Q\rangle$ is given by

$$\langle Q\rangle = \varepsilon^2 \int_0^1 U_{20}(y)\,\mathrm{d}y. \tag{59}$$

Thus, the traveling wave induces a net flow of the liquid, of which the (dimensionless) rate is expressed by Eq. (59). Hence, the net flow is an effect of order ε^2.

4. Results and discussion

In order to estimate quantitatively the effects of various parameters involved in the results of this analysis, the mean velocity at the boundary D_{wall}, the mean velocity perturbation function $G(y)$, the time-averaged mean axial velocity distribution, and the net flow rate are calculated. We are interested in studying the effects of the magnetic parameter M, the permeability parameter of the medium W, the relaxation time τ, the compressibility parameter χ, and the slip parameter K_n on the mean-time average velocity. It is obvious that we have to choose ($\varepsilon < 1$) because we have used the perturbation method with the amplitude ratio (ε) serving as a parameter.

Figures 1(a)–1(e) show the variations of D_{wall} ($= U_{20}(1)$) with wave number α for various values of M, W, τ, χ, and K_n. In Fig. 1(a), it is noticed that M has an increasing effect on D_{wall}. Figures 1(b) and 1(c) show that W and τ both have decreasing effects on D_{wall}. It is also observed from Fig. 1(c) that in the case of Maxwell fluid, D_{wall} is much smaller in magnitude than that in the case of Newtonian fluid ($\tau = 0$). Also, there is a rapid decrease in the value of D_{wall}, which indicates the fact that viscoelastic effects are more pronounced for large values of τ. Figures 1(d) and 1(e) depict that χ and K_n both have decreasing effects on D_{wall} for any value of the wave number α. Moreover, Fig. 1(e) depicts that D_{wall} is bigger in magnitude for the nonslip fluid than for the slip fluid.

Following Fung and Yih,[27] we define the mean velocity perturbation function $G(y)$ as

$$G(y) = \frac{-200}{\alpha^2 R^2}[E(y) - E(1)].$$

Figures 2(a)–2(e) are plotted so as to study the behavior of $G(y)$ with y for various values of the concerned parameters. It is noticed that M, τ, and K_n each have a decreasing effect on $G(y)$ while χ and W each have an increasing effect on it. It is also concluded that $G(y)$ is larger for the Newtonian fluid and becomes smaller for larger values of Maxwell parameter τ, as illustrated in Fig. 2(c). In addition, there is a rapid decrease in the value of $G(y)$. It is also observed that $G(y)$ is at maximum near the center of the channel and remains constant over a certain range of y, as shown in Fig. 2(d); this range decreases by increasing χ. Moreover, Fig. 2(e) shows that the mean velocity perturbation function is bigger in value for the nonslip fluid than for the slip fluid. It is noticed that the flow is symmetric.

Figures 3(a)–3(e) elucidate the variations of the mean velocity distribution with y for various values of the indicated parameters. Figures 3(a) and 3(c) reveal that upon increasing the magnetic parameter and Maxwell parameter, the mean flow distribution decreases and yet we observe a backward flow. Moreover, it is noticed that such a backflow for Newtonian fluid is more than that for the non-Newtonian one, which is a general observation that the velocity decreases with the viscoelastic parameter increasing for viscoelastic fluids. Figure 3(b) shows that the mean velocity distribution increases

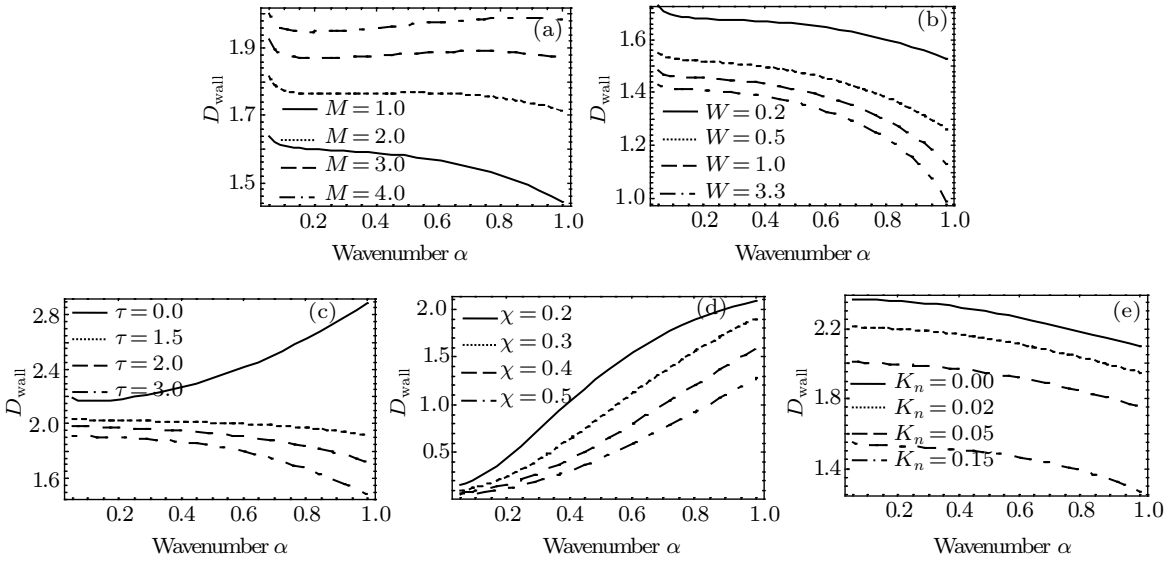


Fig. 1. Variations of $D_{\rm wall}$ with wave number α for $W = 1$, $\tau = 1$, $\chi = 0.001$, $K_n = 0.15$, and $R = 10$ (panel (a)); $M = 0.5$, $\tau = 1$, $\chi = 0.001$, $K_n = 0.15$, and $R = 10$ (panel (b)); $M = 0.5$, $W = 1$, $\chi = 0.001$, $K_n = 0.15$, and $R = 50$ (panel (c)); $M = 2$, $W = 3.3$, $\tau = 1$, $K_n = 0.15$, and $R = 10$ (panel (d)); $M = 1$, $W = 1$, $\tau = 2$, $\chi = 0.001$, and $R = 10$ (panel (e)).

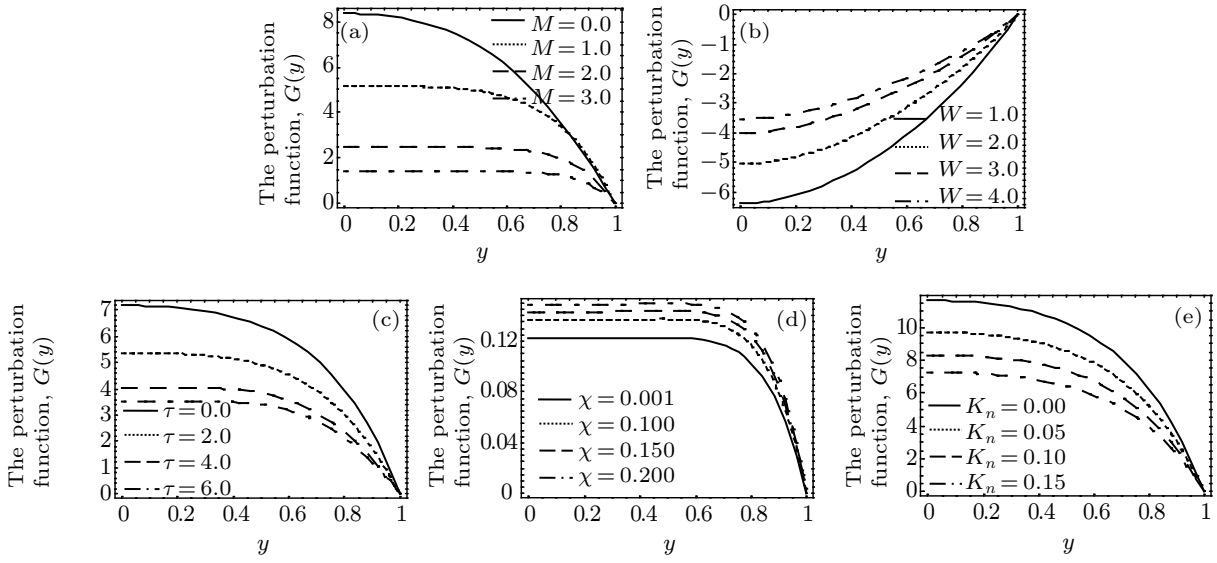


Fig. 2. Variations of the mean velocity perturbation function $G(y)$ for $W = 0.5$, $\tau = 2$, $\chi = 0.3$, $K_n = 0.01$, $R = 10$, and $\alpha = 0.5$ (panel (a)); $M = 0.005$, $\tau = 0.05$, $\chi = 0.01$, $K_n = 0.15$, $R = 10$, and $\alpha = 0.2$ (panel (b)); $M = 0.5$, $W = 1$, $\chi = 0.3$, $K_n = 0.1$, $R = 10$, and $\alpha = 0.5$ (panel (c)); $M = 0.5$, $W = 1$, $\tau = 0.5$, $K_n = 0.15$, $R = 100$, and $\alpha = 0.5$ (panel (d)); $M = 0.5$, $W = 1$, $\tau = 0.5$, $\chi = 0.3$, $R = 10$, and $\alpha = 0.5$ (panel (e)).

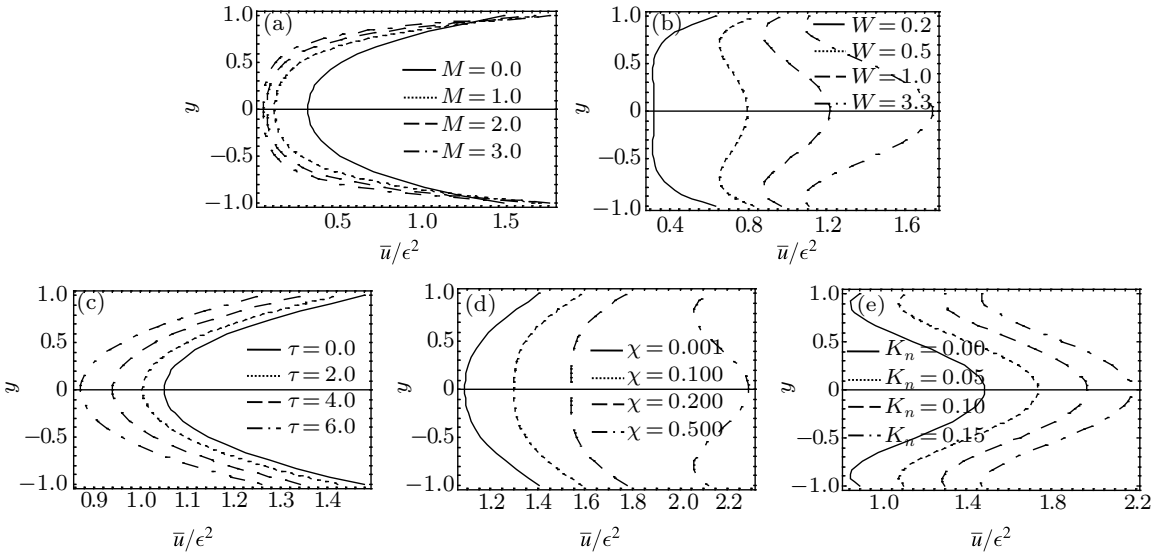


Fig. 3. Variations of the mean-axial velocity distribution for $W=0.2$, $\tau=2$, $\chi=0.1$, $K_n=0.15$, $R=10$, and $\alpha=0.5$ (panel (a)); $M=0.05$, $\tau=0.5$, $\chi=0.9$, $K_n=0.05$, $R=10$, and $\alpha=0.5$ (panel (b)); $M=1$, $W=3.3$, $\chi=0.05$, $K_n=0.05$, $R=10$, and $\alpha=0.5$ (panel (c)); $M=0.01$, $W=3.3$, $\tau=0.5$, $K_n=0.05$, $R=10$, and $\alpha=0.4$ (panel (d)); $M=0.05$, $W=3.3$, $\tau=0.5$, $\chi=0.9$, $R=10$ and $\alpha=0.5$ (panel (e)).

with permeability parameter W increasing; this happens because the permeability parameter allows more quantities of fluid to pass through the pores. Thus, the bigger the permeability, the greater the velocity of fluid is. In addition, Figs. 3(d) and 3(e) show that the mean flow distribution increases with the values of χ and K_n increasing. It is also shown that the mean flow has less magnitude for the nonslip fluid than for the slip fluid.

Figures 4(a)–4(i) show the variations of the net flow rate $\langle Q\rangle$ with χ and α for various values of the parameters M, W, K_n, and τ. We have made several runs of our code for different values of these parameters. We note that M, W, K_n and τ enter into the equations because we have included the nonslip flow through porous medium into the non-Newtonian Maxwell model in the presence of a magnetic field. First, we investigate the effect of M on $\langle Q\rangle$ and we notice that M has a decreasing effect on $\langle Q\rangle$ at any value for χ and α, as shown in Figs. 4(a) and 4(b). In Fig. 4(a), we investigate the dependences of $\langle Q\rangle$ on χ for various values of M. We notice that for $M=1.4$, the net flow rate $\langle Q\rangle$ reaches its maximum at $\chi=0.2$. Further, for $M=2$, the maximum value of $\langle Q\rangle$ occurs at $\chi=0.1$. Moreover, for $M=4$ and $M=6$, we notice that the maximum values of $\langle Q\rangle$ occur at $\chi=0.06$ and $\chi=0.04$, respectively. In Figs. 4(c) and 4(d), we investigate the dependences of $\langle Q\rangle$ on compressibility parameter χ and on wave number α for various values of W. We observe that the flow rate increases with W increasing at any value for χ and α. In Fig. 4(c), we notice that $\langle Q\rangle$ reaches its maximum value at $\chi=0.9$ for all values of W. Figures 4(e) and 4(f) are plotted so as to investigate the dependences of $\langle Q\rangle$ on χ and α for various values of the slip parameter K_n. We set K_n to be different values and investigate the changes induced by the slip parameter. In Fig. 4(e), we observe that the net flow rate decreases by K_n increasing at any value of χ. Moreover, the maximum value for $\langle Q\rangle$ occurs at $\chi=0.14$ for all values of K_n. In Fig. 4(f), we notice that at any value of α, the net flow rate decreases with K_n increasing.

Further, to investigate the dependence of the flow rate $\langle Q\rangle$ on τ, we perform the calculations for a few values of τ. For $\tau=100$, we notice a slight deviation from the Newtonian limiting case (solid line), which translates into shifting the maximum towards larger values of χ, as shown in Fig. 4(g). For $\tau=10^3$ and $\tau=10^4$, we notice a further deviation from the Newtonian flow, which also translates into shifting the maximum towards larger values of χ. We notice that $\langle Q\rangle$ increases as τ increases at any value of χ and that it reaches its maximum value at $\chi=0.9$ for all values of τ. In Fig. 4(h), we investigate the dependences of the flow rate $\langle Q\rangle$ on the parameter α. We observe that at any value of α, the net flow rate increases with τ increasing. We investigate novelties brought about by the introduction of non-Newtonian effects (the appearance of non-zero relaxation time τ) into the model. We treat the latter case, $\tau=10^4$, separately, owing to the appearance of the negative flow rates. In Fig. 4(i), it is shown that for $\alpha\geq 0.48$, $\langle Q\rangle$ becomes negative, i.e., we observe a backflow. We conclude that in this deeply non-Newtonian regime, further $\tau=10^4$, $\langle Q\rangle$ becomes highly oscillatory. However, what is unusual is that we observe the negative flow rates for certain values of α. Obviously, the negative $\langle Q\rangle$ means that flow occurs in the direction opposite to the direction of the propagation of the traveling wave on the channel wall. Oscillatory behavior (the appearance of numerous maxima in the behavior of the physical variable) in the deeply non-Newtonian regime is not new.[28,29] However, the flow of a fluid created by the peristaltic mechanism in the direction opposite to the direction of the propagation of the traveling wave is unusual and should be attributed to a complicated, nonlinear form of the response of a Maxwell fluid to the stress exerted by the wave.

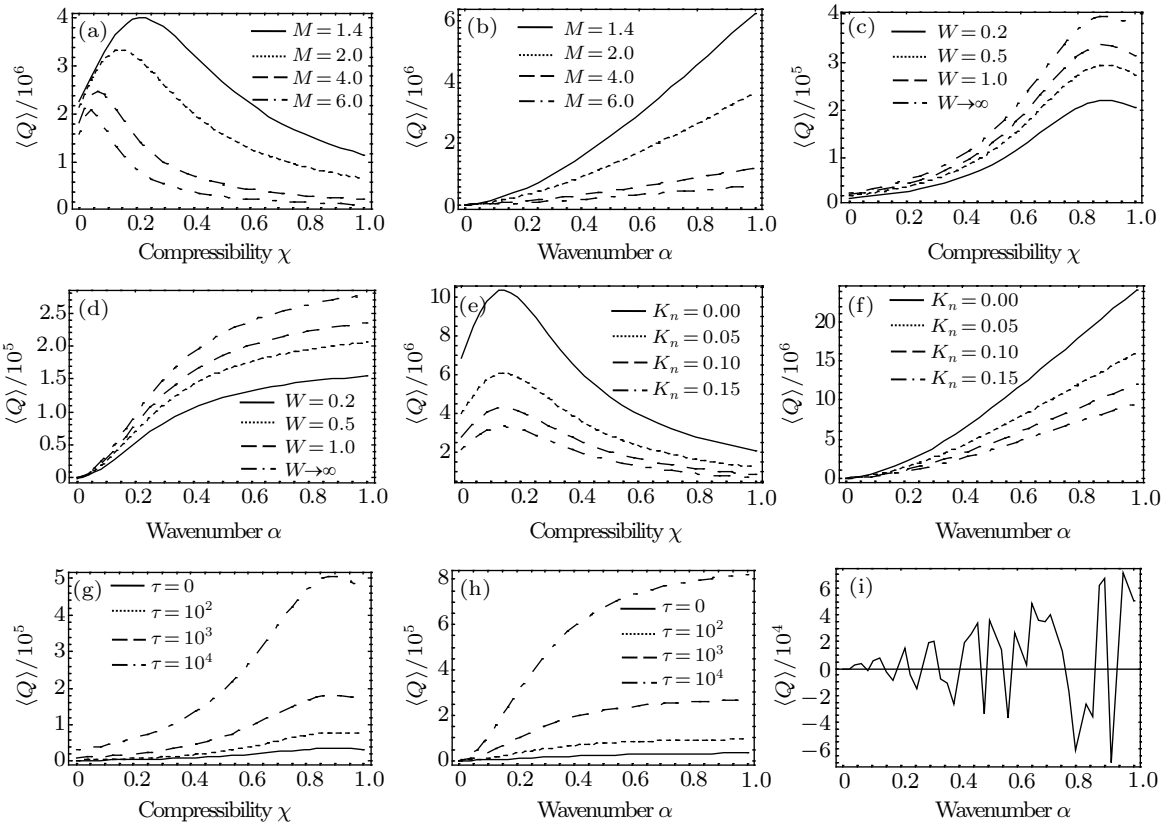


Fig. 4. Dimensionless net flow rate $\langle Q\rangle$ curves for $W=3.3$, $\tau=1000$, $K_n=0.15$, $R=100$, $\varepsilon=0.001$, and $\alpha=0.5$ (panel (a)); $W=3.3$, $\tau=1000$, $K_n=0.15$, $R=100$, $\varepsilon=0.001$, and $\chi=0.6$ (panel (b)); $M=0.2$, $\tau=1000$, $K_n=0.05$, $R=10$, $\varepsilon=0.001$, and $\alpha=0.5$ (panel (c)); $M=0.2$, $\tau=1000$, $K_n=0.05$, $R=10$, $\varepsilon=0.001$, and $\chi=0.6$ (panel (d)); $M=2$, $\tau=10^3$, $W=3.3$, $R=100$, $\varepsilon=0.001$, and $\alpha=0.5$ (panel (e)); $M=1$, $\tau=10^3$, $W=0.5$, $R=100$, $\varepsilon=0.001$, and $\chi=0.6$ (panel (f)); $M=0.2$, $K_n=0.05$, $W=1$, $R=10^4$, $\varepsilon=0.001$, and $\alpha=0.5$ (panel (g)); $M=0.2$, $K_n=0.05$, $W=3.3$, $R=100$, $\varepsilon=0.001$, and $\chi=0.6$ (panel (h)); $\tau=10^4$, $M=0.0002$, $K_n=0.05$, $W=3.3$, $R=10^4$, $\varepsilon=0.001$, and $\chi=0.6$ (panel (i)).

It should be noted that the results of compressible viscous fluid filling the non-porous medium with noncompliant walls of Mekheimer and Abdel–Wahab[4] can be obtained by taking $M=0$, $\tau=0$, and $W\to\infty$ in our investigation. Also, choosing $M=0$, $K_n=0$ and $W\to\infty$ refers to a well-agreed physical situation for compressible fluids as obtained by Tsiklauri and Beresnev.[29] Moreover, our results are in agreement with the results of Eldesoky and Mousa[30] when $M=0$ and $K_n=0$ are taken in our investigation.

5. Conclusions

In this study, the peristaltic flow of a compressible Maxwell fluid induced by a surface acoustic wave in a confined parallel-plane microchannel through a porous medium is discussed in the presence of a constant magnetic field. The problem is discussed only for the free pumping case. The main findings can be summarized as follows.

(i) In the non-Newtonian regime, there is a possibility of a fluid flow in the direction opposite to the propagation of the traveling wave.

(ii) The mean flow at the boundaries, the mean velocity perturbation function $G(y)$ and reversal flow are bigger for Newtonian fluids than for non-Newtonian ones.

(iii) The mean flow at the boundaries, the mean velocity perturbation function $G(y)$, and the reversal flow are bigger in magnitude for the nonslip fluid than for the slip fluid.

(iv) The magnetic field has a decreasing effect on the mean velocity perturbation function $G(y)$, while it has an increasing effect on both the mean velocity at the boundaries and the mean flow.

(v) The Maxwell parameter τ has a decreasing effect on the mean velocity at the boundaries, the mean velocity perturbation function $G(y)$, and the mean flow.

(vi) The permeability parameter W has an increasing effect on the mean velocity perturbation function $G(y)$ and the mean flow, while it has a decreasing effect on the mean velocity at the boundaries.

(vii) The slip parameter K_n has a decreasing effect on the mean velocity at the boundaries and the mean velocity perturbation function $G(y)$, while it has an increasing effect on the mean flow.

(viii) The compressibility parameter χ has an increasing effect on the mean velocity perturbation function $G(y)$, while it has a decreasing effect on both the mean velocity at the boundaries and the mean flow.

(ix) For very low compressibility, the net flow is weakly affected by the magnetic field, permeability parameter, and

Maxwell parameter.

(x) The flow rate for the nonslip flow is higher than that for the slip flow.

(xi) The flow rate for the Newtonian fluid is less than that for the non-Newtonian fluid.

(xii) The results for the Newtonian incompressible fluid with a magnetic field and porous medium can be recovered if the compressibility and slip parameters vanish.

References

[1] Beil F W, Wixforth A and Blick R H 2002 *Physica E* **13** 473
[2] Chu K H W 2000 *Meccanica* **35** 69
[3] Esashi M, Minami K and Ono T 1998 *Condens. Matter News* **6** 31
[4] Mekheimer Kh S and Abdel–Wahab A N 2011 *Inc. Numer. Methods Partial Diff. Eq.* **27** 621
[5] Zhang C B, Chen Y P, Shi M H, Fu P P and Wu J F 2009 *Acta Phys. Sin.* **58** 7050 (in Chinese)
[6] Chu K H W 2001 *Eur. Phys. J. Appl.* **13** 147
[7] Chu K H W 2002 *Phys. Scr.* **65** 283
[8] Chu K H W and Fang J 2000 *Eur. Phys. J. B* **16** 543
[9] Komvopoulos K 1996 *Surface Engineering and Microtribology for Microelectromechanical Systems* **200** 305
[10] Hayat T, Javed M and Asghar S 2008 *Phys. Lett. A* **372** 5026
[11] Mekheimer Kh S and Abd Elmaboud Y 2008 *Phys. Lett. A* **372** 1657
[12] Mekheimer Kh S and Abd Elmaboud Y 2008 *Physica A* **387** 2403
[13] Mekheimer Kh S and Abd Elmaboud Y 2008 *J. Appl. Bionic Biomech.* **5** 47
[14] Ali N, Hayat T and Asghar S 2009 *Chaos, Solitons and Fractals* **39** 407
[15] Elkoumy S R, Barakat E S B and Abdelsalam S I 2012 *Transp. Porous Med.* **94** 643
[16] Hayat T, Ali N and Asghar S 2007 *Phys. Lett. A* **363** 397
[17] Mekheimer Kh S 2004 *Appl. Math. Comput.* **153** 763
[18] Elshehawey E F, Sobh A M and Elbarbary E M E 2000 *J. Phys. Soc. Jpn.* **69** 401
[19] Lukashev E A 1993 *Kaledney J.* **55** 109 (in Russian)
[20] Raptis A, Perdikis C and Tzivanidis G 1981 *J. Phys. D* **14** 99
[21] Raptis A and Perdikis C 1983 *Int. J. Eng. Sci.* **21** 1327
[22] Aarts A C T and Ooms G 1998 *J. Eng. Math.* **34** 435
[23] Hayat T, Khan Y, Mekheimer Kh S and Ali N 2010 *Inc. Numer. Methods Partial Diff. Eq.* **26** 345
[24] Mekheimer Kh S 2003 *Arab. J. Sci. Eng.* **28** 183
[25] Mekheimer Kh S 2004 *Appl. Math. Comput.* **153** 763
[26] Mekheimer Kh S and Abdel–Wahab A N 2012 *J. Aerospace Eng.* **25** 660
[27] Fung Y C and Yih C S 1968 *J. Appl. Mech.* **35** 669
[28] Qi Q, Johnson R E and Harris J G 1995 *J. Acoust. Soc. Am.* **97** 1499
[29] Tsiklauri D and Beresnev I 2001 *Phys. Rev. E* **64** 03630
[30] Eldesoky I M and Abdallah A M 2009 13*th International Conference on Aerospace Sciences & Aviation Technology* (Egypt: Military Technical College)